

Simplified, Rational Approach to Falling Weight Deflectometer Data Interpretation

DIETER F. E. STOLLE AND FRIEDRICH W. JUNG

The authors present a simple elastostatic approach to estimate a suitable subgrade modulus from falling weight deflectometer (FWD) data. An effective surface modulus is defined on the basis of Boussinesq-Newmark equations. Deviations between the model assumptions and actual in situ conditions are reflected in the effective surface modulus variation with radius. The variation indicates which sensor readings are suitable for backcalculation. The presence of a shallow bedrock, increase in subgrade modulus with depth, or anisotropic properties may lead to nonconservative estimates of subgrade modulus. Assuming that the deflections at the subgrade surface (not directly under the load) may be approximated by the surface deflections, the Boussinesq-Odemark equations are used to define an effective subgrade modulus. In order to determine the subgrade modulus, the equivalent thickness of the pavement structure, which reflects pavement stiffness, is estimated by fitting preselected normalized deflections. Given the equivalent thickness, an effective subgrade modulus profile is established, from which a design subgrade modulus may be determined. An example using data of the Canadian Strategic Highway Research Program (C-SHRP) demonstrates the approach. The uniformity of the subgrade at the C-SHRP site is studied by considering the spectral density functions of the FWD time histories. The group velocity is used to define a weighted average profile modulus. The profile moduli of the two sections studied were higher but consistent with subgrade moduli estimated using elastostatic analysis.

Pavements deteriorate gradually over many years. To assist in the decision making with respect to the allocation of funds and resources for the maintenance and rehabilitation of the aging highway network, the highway engineer is finding it necessary to rely more and more on nondestructive testing (NDT) techniques for evaluating the structural integrity of pavement structures. A popular NDT approach is falling weight deflectometer (FWD) testing, together with the interpretation of the surface deflection data via rational analysis. FWD testing is reliable, quick to perform, and its data can provide the engineer with an objective estimate of structural pavement stiffness.

A key component in the interpretation of FWD data for evaluating the structural integrity of pavements is backcalculation analysis. Unfortunately backcalculation problems are often ill-conditioned and their solutions are not unique, even under ideal conditions (1,2). These difficulties are aggravated

by the fact that the mechanical models often used in backcalculation analyses do not properly take into account the material properties and the dynamic nature of the FWD load. Recognizing the analysis limitations, Lytton et al. (3) developed an expert systems environment to help provide more realistic interpretation of FWD data.

It is clear that the use of more realistic mechanical models is most desirable from a fundamental point of view. Although many advanced models are available, the potential gains achieved from these models are most often undermined by the lack of input data, which is required to properly define the boundary-valued problem, and by the increased difficulty to converge to physically admissible solutions. Furthermore, one cannot afford to use computationally intensive models within a pavement management environment in which several thousand calculations may be made using the data collected during FWD testing. Examples of data that are often not available include: accurate thickness of each layer, spatial variation of subgrade materials and moisture content, and stress history of subgrade material.

The objective of this paper is to present a simple, "workhorse" approach for characterizing pavement structures using FWD data. Implicit in the approach is the understanding that insufficient information generally exists to properly define a pavement structure, boundary-valued problem. Consequently, FWD data are interpreted by implicitly taking into account why backcalculated, effective moduli deviate from expected, idealized trends. To provide additional information on the variation of subgrade properties, it is demonstrated how spectral analysis techniques may be used to investigate the uniformity of the subgrade along the road. Although considerable literature exists on backcalculation, only those papers considered to be most relevant to this contribution are referenced.

MECHANICAL MODELS

A typical pavement structure, shown in Figure 1, consists of a prepared subgrade over which granular base and asphalt concrete courses are constructed. Computer programs developed for pavement analysis, such as BISAR and ELSYM5, generally assume linear elastic theory where the upper, parallel layers extend to infinity in the horizontal plane, and the subgrade is assumed to be semi-infinite. These programs are considered to provide exact solutions. One must remember,

D. F. E. Stolle, Department of Civil Engineering and Engineering Mechanics, McMaster University, Hamilton, Ontario, Canada L8S 4L7. F. W. Jung, Pavements and Roadway Section, Research and Development Branch, Ministry of Transportation of Ontario, Downsview, Ontario, Canada M3M 1J8.

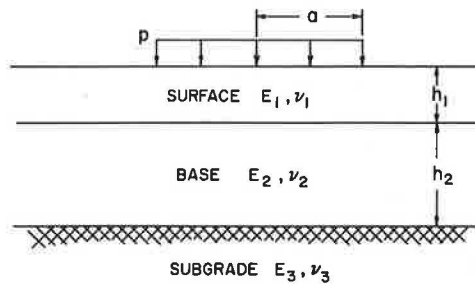


FIGURE 1 Typical pavement structure.

however, that "exact" refers to the solution of idealized problems.

To more realistically take into account the stress-dependent nature of the pavement and subgrade materials, models have been developed within the finite element framework. Although these models help provide a better understanding of a pavement's response to surface loading in a qualitative sense (4), their use within a backcalculation environment will not necessarily provide better quantitative solutions because the input data with respect to distribution of properties within the subgrade must still be assumed. In other words, these models still provide an idealization. Furthermore, because of the nature of the finite element approximation, it is not clear, a priori, how sensitive a backcalculated solution is to discretization.

Realistic analysis of pavement structures, for the purpose of design or evaluation of in situ properties by means of backcalculation, is complicated by the complex properties of the materials and their distribution. All models provide solutions that deviate from the actual in situ behavior. As a model becomes more complex, it becomes more difficult to keep track of the parameter(s) responsible for any deviation between ideal and actual behavior. As a result, the approach described here emphasizes the use of simple models. However, an appropriate mechanical model should reflect the phenomenon being studied, and backcalculation should not attempt to extract more information than is provided by what is actually known from the input data.

The simplest model that was considered is a flexible circular plate of radius a and uniform pressure p , supported by a semi-infinite, linear elastic homogeneous half space. Neglecting the friction that may develop between the plate and foundation and assuming isotropic properties it is possible to evaluate an effective surface modulus (E_{eff}) (5,6) using

$$E_{eff}(r) = \frac{p(1 - \nu^2)}{w(r)} a \Omega_1(r/a) \quad (1)$$

where

ν = assumed Poisson's ratio for the half space,
 r = radius at which the vertical deflection $w(r)$ is calculated, and

$\Omega_1(r/a)$ = a shape function.

If the in situ measurements correspond to a problem that satisfies all model assumptions exactly, E_{eff} should be independent of r . Because the model is only an approximation, E_{eff} is not constant. The relationship between E_{eff} and r pro-

vides the engineer information with respect to the variation of material stiffness with depth.

A second model is introduced that recognizes that the pavement structure is constructed with materials that have elastic moduli higher than that of the subgrade. Using the Boussinesq-Odemark methodology (6), the displacement [$w_s(r)$] at the subgrade level may be approximated as

$$w_s(r) = \frac{P(1 + \nu)}{2\pi E_3 h_e} \Omega_2(r/h_e) \quad (2)$$

where h_e = equivalent thickness:

$$h_e = 0.9 (h_1^3 \sqrt{E_1/E_3} + h_2^3 \sqrt{E_2/E_3}) \quad (3)$$

Ω_2 = shape function:

$$\Omega_2(r/h_e) = \frac{1}{R^3} + \frac{2(1 - \nu)}{R} \quad (4)$$

where

$R = [1 + (r/h_e)^2]^{1/2}$,
 P = applied load, and
 E_3 = subgrade modulus.

The elastic moduli E_1 and E_2 and thicknesses h_1 and h_2 are defined in Figure 1. The definition for equivalent thickness in Equation 3 assumes that the Poisson's ratio (ν) is the same for all layers. Equation 2 may be used to estimate the surface deflection [$w(r)$], provided that the vertical strains in the pavement structure are small. This is generally true for thin, stiff layers or if deflections are calculated at r greater than $2a$. If Equation 2 is inverted, one may evaluate an effective subgrade modulus (E_s), provided that h_e is known or can be estimated. Similar to E_{eff} , the functional relationship between E_s and r provides the engineer with information on the variation of material stiffness with depth.

LIMITATIONS OF MODELS

The FWD is an instrument that measures the deflection history at various sensors caused by an impulse load created by a falling weight. The time history of deflections arising from an FWD test is shown in Figure 2. The load is distributed over a circular plate of 30 cm diameter and thus resembles, also in its duration, a passing heavy single-tire wheel load from a truck. The peak deflections measured at various distances from the load only superficially resemble the deflection basin created by an equivalent elastostatic load. Elastodynamic analysis (7,8) indicates that the shape of the deflection bowl defined by peak deflections is different from that corresponding to an elastostatic load. Consequently, a systematic error is introduced to subgrade modulus estimates when elastostatic models are used for backcalculation. A factor not considered with respect to load application is the pressure distribution under the plate. Although the effect of the pressure distribution on effective moduli estimates may be important in the immediate vicinity of a plate resting on a weak pavement structure, its effect is diminished as pavement stiff-

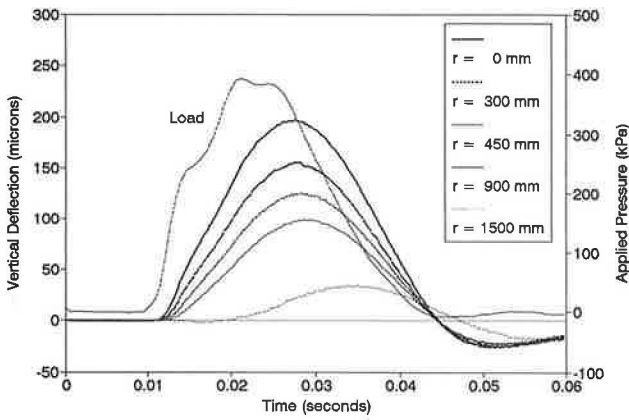


FIGURE 2 Typical FWD load and deflection histories.

ness or the radius at which the displacement is observed increases.

Real pavement and subgrade materials exhibit nonlinear stress-strain behaviors that are sensitive to stress level, temperature, moisture content, and loading history (3,9). To compound analysis difficulties, the properties are not uniform, and continuum mechanics concepts do not apply to the analysis of cracked or broken-up pavements. Consequently, the use of Equations 1 and 2 must be accompanied by the understanding that the moduli associated with these equations are not material properties, but model parameters which vary with time (10). These parameters, which directly reflect material properties, undergo an evolution influenced by environmental factors and traffic history.

The difficulty of incorporating the evolution of properties into a model can be easily appreciated by considering what happens during the development of residual stresses as a result of plastic deformations induced by a heavy load (4) and subsequent stress relief due to creep as temperatures rise. Although it may be possible to follow such a process for one or two load applications, it is not possible to do so for the general random nonlinear loading process that is encountered in practice. Fortunately an NDT program can provide the engineer with some of the information lacking when the evolution details of material properties in a mechanical model are neglected.

IDEALIZED EXAMPLE

A comparison of computer-generated and measured deflection bowls clearly indicates that differences exist between actual field conditions and what is assumed for modeling. In order to investigate possible reasons for the observed differences, an idealized two-layer pavement was studied; the effects of bedrock location and dynamic impact loading were taken into account. The problem profile consisted of a pavement with an elastic modulus of 2,250 MPa and Poisson's ratio of 0.35, supported by a homogeneous subgrade with an elastic modulus of 45 MPa and a Poisson's ratio of 0.50. The elastostatic deflection bowls were generated using ELSYM5.

The elastodynamic analyses were completed using a discrete layer approach similar to that described elsewhere (7). The version of the model adopted for this study, however, treated the pavement as a Kirchhoff plate and the subgrade

as a semi-infinite halfspace. The analysis procedure was based on a Galerkin approach in which Burmister's static solution (11), together with a Bessel-Fourier expansion, provided an interpolation function for displacements in the subgrade. The Burmister solution was assumed to be acceptable as an interpolation function because the FWD load is dominated by low frequency content. In order to take advantage of Bessel function orthogonality properties, the load was also expressed by a Fourier series approximation, thereby permitting an uncoupled time-domain solution for each term of the series. The net displacement response at a point was obtained by linearly superimposing the appropriate contribution from each solution. When generating the elastodynamic deflection bowls, the FWD impact load was applied as a half-sine wave over a time interval of 0.025 sec, and a unit weight of 20 kN/m³ was assumed.

The effective surface modulus profiles using data from the elastostatic analyses are summarized in Figures 3 and 4, and the profiles obtained from deflection bowls generated by the discrete layer model are compared in Figure 5. Figure 3 clearly shows that an increase in effective modulus, when real data are used, can be attributed to the presence of bedrock at shallower depths. The strength of the effective modulus increase with radius depends on the subgrade thickness (*H*). As *H* decreases, both the minimum effective modulus and rate of increase of the distant effective moduli increase.

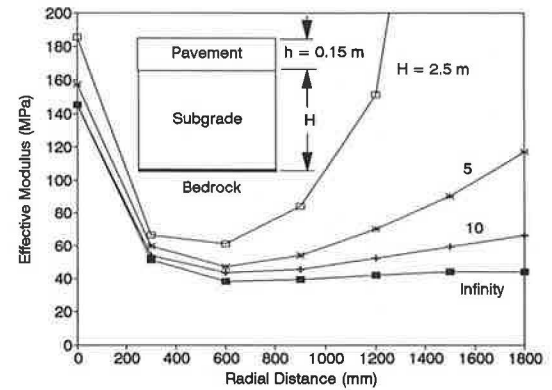


FIGURE 3 Influence of subgrade thickness (*H*) on effective surface modulus.

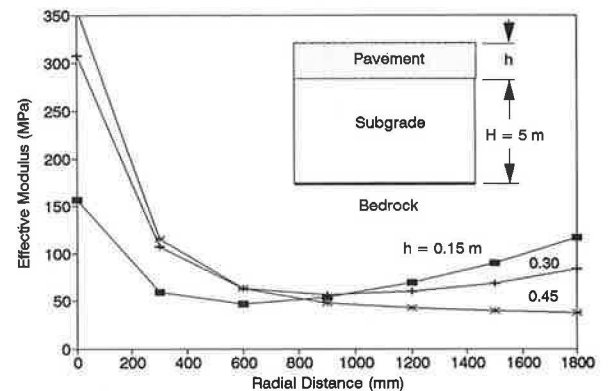


FIGURE 4 Influence of pavement thickness (*h*) on effective surface modulus.

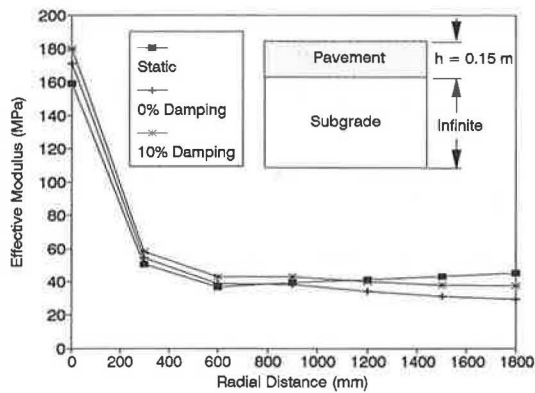


FIGURE 5 Influence of dynamic loading on effective surface modulus.

Although not shown, the increase in effective modulus at larger radii can also be explained if the subgrade modulus increases with depth (6) or if the subgrade properties are anisotropic (12). The presence of bedrock at shallow depths may be regarded as providing a sudden increase in subgrade stiffness. Owing to the sensitivity of the outside sensors to material properties deeper within the subgrade, it is clear that the sensors farther away from the load may not be suitable for estimating an average subgrade modulus that is representative of that portion of the subgrade that has the greatest impact on the life of a pavement.

As expected, the effective modulus profile, for the case in which the subgrade extends to infinity, asymptotically approaches 45 MPa as the radial distance from the load increases. The dip below 45 MPa at $r = 600$ mm, and the subsequent gradual increase of E_{eff} , is a result of the Poisson's ratio of the pavement being different from that of the subgrade. A Poisson's ratio of 0.5 was used to estimate all effective surface moduli. Had the Poisson's ratio of the pavement, $\nu_1 = 0.35$, been substituted into Equation 2 for the point at $r = 600$ mm, the effective modulus would have been slightly larger than 45 MPa. If effective moduli are estimated using idealized deflection bowls in which all layers have identical Poisson's ratios, the minimum effective modulus is attained at $r \rightarrow \infty$ (5).

Figure 4 shows that the minimum effective surface modulus occurs at a larger radial distance as the thickness of the pavement increases. For the idealized two-layer problem the radius at which E_{eff} is a minimum corresponds approximately to h_e . As the minimum E_{eff} is pushed further away from the load, the positive slope at the outer sensors is decreased.

When the deflection bowl data from the elastodynamic analysis are used, the effective surface modulus decreases below 45 MPa as r increases, as shown in Figure 5. This is not surprising because the decay rate with respect to radius of a deflection bowl defined by a propagating wave is less than that corresponding to an elastostatic deflection bowl (7). Although it is clear that the dynamic nature of the FWD load has an influence on effective moduli predictions, these effects may be quite small when compared with those associated with subgrade modulus increase with depth or anisotropic soil properties.

The results from the idealized two-layer problem suggest that the effective surface modulus variation with radius may

be used to characterize a pavement-subgrade profile: (a) radial distance to the minimum E_{eff} is proportional to h_e ; (b) minimum E_{eff} provides a ballpark stiffness estimate of the average subgrade modulus in the vicinity of the load; and (c) taking into account pavement stiffness, dE_{eff}/dr at larger values of r may indicate how subgrade modulus increases with depth. It appears that the effects of the unknowns associated with subgrade modeling and the dynamic nature of the FWD load are relatively small, provided that the sensor readings directly under the load and on the positive dE_{eff}/dr branch are not used in backcalculation.

The use of the outside sensors can lead to nonconservative estimates in subgrade modulus. To compensate for the differences between the assumed and the actual conditions, Jung (13) developed a curve-fitting strategy to permit the use of outside sensors for backcalculation. The strategy incorporates the peak deflections from the outside three or four sensors by introducing a power law fit

$$\log(E_{eff}) = (\eta - 1) \log(r) + C \quad (5)$$

where E_{eff} corresponding to radius r is obtained from the deflection data using Equation 1, and η and C are constants evaluated from regression analysis. It is suggested that a representative subgrade modulus may be estimated from Equation 5 by calculating E_{eff} at a radius of 0.75 m (13). Analyses involving actual FWD data indicate that the error of fit obtained, when trying to fit the last three or four sensor readings, may provide a measure of pavement condition (i.e., badly cracked or broken pavements have high errors of fit, whereas pavements in good condition have low errors of fit) (5).

BACKCALCULATION STRATEGY

Various backcalculation strategies are used for solving the inverse problem. The approach most often adopted involves the following steps:

1. Estimate the seed moduli via some approximate strategy,
2. Predict a deflection basin using estimated moduli,
3. Compare predicted and measured deflection basins,
4. Adjust layer moduli through a search technique to reduce differences between measured and predicted displacements, and
5. Repeat Steps 2 to 4 until error between the two deflection basins is within an allowable tolerance.

Regardless of which procedure is used, solutions are not unique and engineering judgment is required to determine whether the predictions are reasonable.

The backcalculation procedure proposed here is simplified significantly by absorbing the effect of the pavement structure on displacements through a single parameter: h_e . The solution procedure is based on rewriting Equation 2 as

$$\frac{w(r)}{w(r_n)} = \frac{\Omega_2(r/h_e)}{\Omega_2(r_n/h_e)} \quad (6)$$

where r_n is the radius corresponding to the sensor for which deflection is used to normalize the deflection bowl data. Tak-

ing into account the results of the idealized example of the previous section and form of Equation 6 leads to the following simple backcalculation strategy:

1. Find the sensor n at which E_{eff} is a minimum,
2. Normalize deflections using sensor n ,
3. Using sensors $i = 2$ to n , find h_e that provides the best root mean square fit to Equation 6,
4. Using optimum h_e , calculate E_s at each sensor to provide an effective subgrade modulus profile, and
5. Estimate the design subgrade modulus from the effective subgrade modulus profile.

The purpose of normalizing the data is to eliminate one unknown, the subgrade modulus, which for Figure 1 corresponds to E_3 . Determining optimum h_e is equivalent to finding a function that best fits the shape of the deflection bowl, which is sensitive to the properties of the pavement structure. It is recommended that the first sensor not be used because a sufficiently large portion of the measured displacement may be due to pavement layer straining that is not taken into account in Equation 2. For pavements with large h_e it may also be necessary to avoid using the second sensor deflection because the error, associated with the assumption that the surface deflection is approximately the same as the subgrade deflection, may also be greater than 10 percent.

PROPAGATION OF ERRORS

As indicated previously, although it is tempting to suggest that more realistic modeling could improve the predictions of the layer moduli, the lack of sufficient input data would most likely undermine the accuracies attainable with more realistic modeling. On the other hand, approximations introduce systematic errors to the predictions owing to incompatibility between model and data. Work by Stolle (2) demonstrates that simplifications introduced for material modeling of the subgrade can have a significant influence on the prediction of the pavement structure moduli. This section briefly addresses this theme with respect to Equation 2.

The error analysis is simplified by considering only sensitivities at $r = 0$ for a two-layer problem. Given that the operator Δ refers to an incremental change, first order expressions for error estimates

$$\left| \frac{\Delta h_e}{h_e} \right| = \left| \frac{\Delta w}{w(0)} \right| + \left| \frac{\Delta E_3}{E_3} \right| \quad (7)$$

$$\left| \frac{\Delta E_1}{E_1} \right| = 3 \left| \frac{\Delta w}{w(0)} \right| + 2 \left| \frac{\Delta E_3}{E_3} \right| + 3 \left| \frac{\Delta h_1}{h_1} \right| \quad (8)$$

may be obtained by using a truncated Taylor's expansion for Equation 2. It should be noted that implicit in the error equations is the assumption that $w(0) \approx w_s(0)$. From Equation 8 it is clear that an error associated with displacement, subgrade modulus, or layer thickness as a result of the model not fitting the data properly amplifies the relative error associated with the pavement modulus. For example, a 10 percent error in both subgrade modulus and pavement thickness could pro-

vide, to the first order, a 50 percent error in the estimate of E_1 . At the same time, the relative error associated with h_e , which indirectly provides a measure of pavement stiffness, is no greater than that of the subgrade modulus. This suggests that it may be more advantageous to deal with h_e instead of E_1 . Besides, an estimate of E_1 is not required to evaluate key diagnostic parameters such as the radial tensile strain at the bottom of the asphalt layer or maximum compressive strain at the surface of the subgrade (13).

TEMPERATURE ADJUSTMENTS

All primary response parameters should be adjusted to a standard reference state of temperature, moisture condition, and loading frequency (9). Of these three variables, temperature adjustment is most critical because the asphalt concrete temperature can change significantly during the day. This makes it difficult to meaningfully compare pavement stiffness predictions from the various test sections that may be located along the same road. Various relationships exist, however the one adopted by Jung (13) is followed here to demonstrate how the equivalent thickness of an asphalt layer is influenced by temperature changes. Given that the temperature dependence of the elastic modulus of asphalt concrete may be approximated as

$$E_1 = E_1^s \exp[k(T - T_s)] \quad (9)$$

where

$$\begin{aligned} E_1^s &= \text{asphalt concrete modulus at temperature } T_s, \\ T - T_s &= \text{temperature difference (degrees Celsius), and} \\ k &= \text{a coefficient.} \end{aligned}$$

The equivalent thickness of the asphalt concrete h_e^a varies according to

$$h_e^a \propto \exp\left[\frac{k}{3}(T - T_s)\right] \quad (10)$$

It should be noted that Equation 10 follows naturally from Equation 9 when one considers the definition for equivalent thickness (see, for example, Equation 3). As shown in Equation 10, h_e^a is not as sensitive to temperature change as the asphalt concrete modulus. Because h_e^a is only a portion of the overall h_e , the temperature change effects may, in some cases, be neglected. For cases in which it cannot be neglected (e.g., extreme temperature differences), an assumption must be made with respect to the asphalt concrete modulus, provided that the asphalt concrete is not severely cracked. If a pavement is severely cracked, a temperature adjustment is meaningless.

CASE HISTORY

One of the C-SHRP test sites is located on Highway 80 south-east of Sarnia. Although the highway was relatively smooth to drive on, the pavement was severely cracked and was therefore rehabilitated with an overlay during the summer of 1989. The pavement profile of Section A consists of a 90 mm bi-

tuminous overlay, 140 mm broken bituminous layer, and 280 mm of Granular A and 560 mm of Granular C sand. The effective modulus profiles at Sections 0.00 and 0.08 are summarized in Figure 6.

The effective moduli were calculated assuming $\nu = 0.5$. The equivalent thicknesses at Sections 0.00 and 0.08 were estimated to be 1005.4 mm and 945 mm, respectively. The slightly lower subgrade moduli shown in Figure 6 for Section 0.00 may, in part, be attributed to the slightly higher h_e at this section. It is clear from this figure that Equation 2 largely filters out the effect of the pavement structure on the effective subgrade modulus estimates. For both these sections, the minimum effective surface modulus, which occurs at $r = 900$ mm, is close to the effective subgrade modulus. A representative subgrade modulus that is assumed to correspond to the deflection at which E_{eff} is minimum is approximately 75 to 80 MPa. The lower subgrade moduli in the vicinity of the load are attributed to systematic errors associated with neglecting the strain in the pavement structure. Farther away, both the effective surface and subgrade moduli merge, as anticipated. The positive increase in the effective moduli at the distance sensors is attributed to the stress-dependence of the subgrade modulus, which would increase with depth. The use of correlation techniques for studying the stiffness increase with depth is discussed briefly in the next section.

CORRELATION ANALYSIS OF FWD DATA

The analysis methodology up to this point has only made use of the peak deflections. In correlation analysis, more often referred to as spectral analysis, the full time history at each sensor, exemplified in Figure 2, is used in order to extract more information. Owing to the nature of FWD load and location of sensors, some constraints complicate the interpretation of the data: (a) low frequencies (0 to 100 Hz) are excited, and consequently only properties in the subgrade can be adequately characterized; and (b) sensors are located in "near field," where Rayleigh waves are not yet fully developed. Because the waves are not fully developed, models that are advanced and more computationally intensive (14) are required to exploit the information provided by the FWD data.

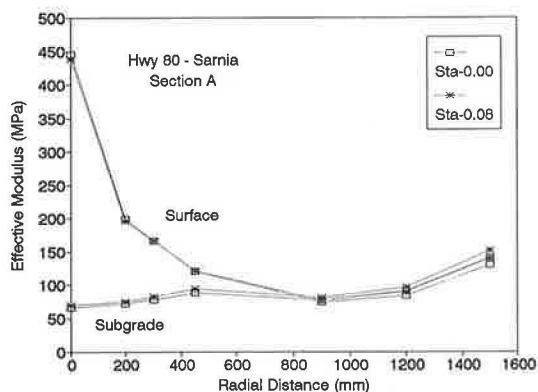


FIGURE 6 Summary of effective surface and subgrade moduli for Sections 0.00 and 0.08, C-SHRP site.

For the purposes of this paper, the objective of correlation analysis is to provide additional information on the uniformity of properties over a region. An important aspect of this approach is that the time lag (τ) in response between two sensors is sensitive to the material properties of the underlying media. Given that the time histories of two sensors are defined by

$$\begin{aligned} x(t) &= w(r_1, t) - \bar{w}(r_1) \\ y(t) &= w(r_2, t) - \bar{w}(r_2) \end{aligned} \quad (11)$$

where $\bar{w}(r_i)$ refers to average values of the deflection history $w(r_i, t)$ at sensor i over a time period T , a covariance function $C_{xy}(\tau)$ may be defined as

$$C_{xy}(\tau) = \frac{1}{T} \int_0^T x(t)y(t + \tau) dt \quad (12)$$

or when working with discrete Fourier transforms (15) as

$$C_{xy}(\tau) = \sum_k A_k \cos(2\pi f_k k\tau + \theta_k) \quad (13)$$

The amplitude A_k and phase lag θ_k are components of the cross-spectral density function (cross-spectrum). The fundamental frequency is given by $f_1 = 1/T$. The correlation coefficient function $\rho_{xy}(\tau)$, which is a normalized equivalent of $C_{xy}(\tau)$, satisfies the constraint $|\rho_{xy}(\tau)| \leq 1$ (15). As with the correlation coefficient used in statistics, $|\rho_{xy}(\tau)| = 1$ implies perfect correlation between two variables that are related through a linear operator.

The phase lag τ_m , which maximizes $\rho_{xy}(\tau)$, can be used to define the group velocity $v_G = \Delta r/\tau_m$, where Δr is the distance between both sensors. Instead of following the usual practice, where the phase velocity v_k corresponding to frequency $f_k = kf_1$ is evaluated for each k in order to estimate the elastic modulus variation with depth (16), the group velocity is used to estimate a weighted average profile modulus

$$E_{av} = 1.21\bar{\rho}v_G^2 \cdot (1 + \nu) \quad (14)$$

where $\bar{\rho}$ is the average density of the subgrade.

The analysis of a semi-infinite halfspace indicates that most of the energy associated with a surface (Rayleigh) wave is concentrated in a zone one wavelength wide (17). Assuming that v_G corresponds to the frequency f_G whose term dominates $\rho_{xy}(\tau)$, then a crude approximation for the zone, to which the average E_{av} applies, may be defined by $\lambda_G = v_G/f_G$. Implicit in Equation 14 is the understanding that λ_G is much larger than the thickness of the stiffer asphalt concrete layer. This constraint is required because the presence of a pavement alters the surface wave velocity. As the wavelength increases the influence of the pavement decreases.

The C-SHRP data were analyzed using the correlation procedure described in this section. The correlation was carried out between Sensors 5 and 7, which were located 900 and 1500 mm away from the load, respectively. The data were sampled at a rate of 0.2 msec for 60 msec. Because discrete Fourier transforms assume that the input is periodic, an additional 724 points consisting of zeros was added at the end of the time-history records to ensure a reasonable transfor-

mation of the nonperiodic data. The results are summarized in Figures 7 and 8.

Figure 7 compares the variation in amplitude and phase angle for both sections. The dominant frequencies for Sections 0.00 and 0.08 are approximately 15 and 10 Hz, respectively. The concave upward increase in phase angle with respect to frequency increase suggests that the elastic modulus increases with depth, which is consistent with the effective modulus profiles. Although the overall phase angle profiles for these sections are similar, the fact that they are not the same indicates that the variations in stiffness with depth may not be identical. The largest differences between the two occur in the frequency range of 35 to 45 Hz, which corresponds to properties close to the pavement structure. The larger phase angle at 44 Hz for Section 0.08 may reflect the fact that the old pavement under the overlay at this section is severely cracked.

Using the data from the correlation coefficient functions shown in Figure 8, the profile modulus E_{av} for Sections 0.00 and 0.08 are estimated to be 113 and 122 MPa, respectively. These estimates are based on an average unit weight of 20 kN/m³ and Poisson's ratio of 0.5. If one were to further assume that the sampling depth is approximately $\lambda_G/2$, then these moduli would correspond to depths of 4 and 6.5 m, respectively. Although these figures are only approximate, the values for E_{av} are consistent with the effective subgrade modulus

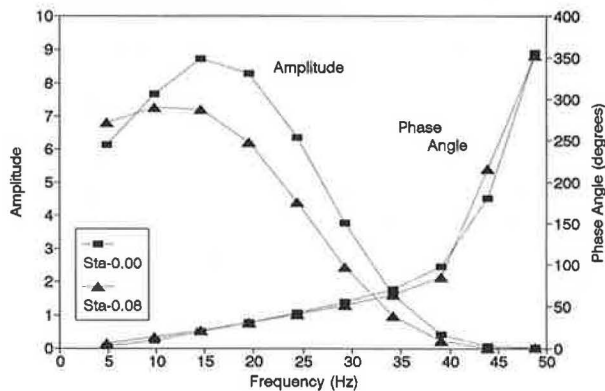


FIGURE 7 Cross-spectrum from FWD data for Sections 0.00 and 0.08, C-SHRP site.

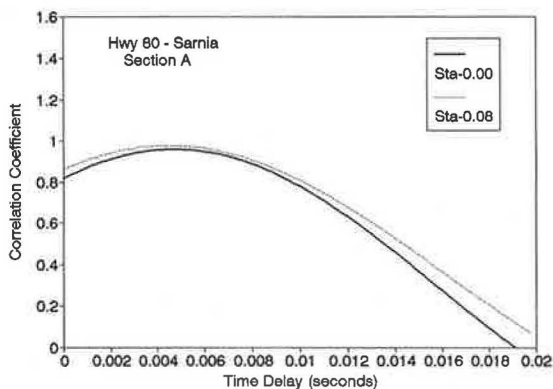


FIGURE 8 Correlation coefficient functions from FWD data for Sections 0.00 and 0.08, C-SHRP data.

predictions shown in Figure 6. For both spectral analyses, the maximum ρ_{xy} is close to one, which confirms an excellent correlation between the behaviors at the two sensors.

CONCLUDING REMARKS

Owing to the complex properties of pavements and subgrade materials, a realistic, accurate stress analysis of a pavement structure is difficult. Systematic errors associated with back-calculated moduli are introduced when imperfect mechanical models are forced to fit in situ data. Although it is desirable to accurately model pavements to obtain a better understanding of stress distributions in these structures, more accurate mechanical modeling, when used in a backcalculation environment, will not necessarily lead to better estimates of in situ properties. As a result, the approach advocated here is to use simple models. When these models are used, estimates of appropriate in situ subgrade moduli are possible through recognition of the reasons for the deviations between the expected and actual modulus predictions.

Emphasis has been placed on estimating subgrade modulus and the apparent stiffness of a pavement structure via the concept of equivalent thickness. It has been shown by using the effective modulus profiles and considering the cospectrum that the properties of a real subgrade vary, as expected. Because errors associated with subgrade modeling can amplify errors associated with the pavement structure moduli predictions, these predictions are considered to be unreliable. Taking this into account and the fact that continuum concepts are no longer applicable to cracked pavements, it is suggested that the effective thickness may provide a better measure of a pavement structure's integrity.

ACKNOWLEDGMENTS

The work reported in this paper was supported by the Ministry of Transportation of Ontario and the National Sciences and Engineering Research Council of Canada. The field data were supplied by D. Hein of Dynatest Canada.

REFERENCES

1. D. Stolle and D. Hein. Parameter Estimates of Pavement Structure Layers and Uniqueness of the Solution. In *Nondestructive Testing of Pavements and Backcalculation of Moduli* (A. J. Bush III and G. Y. Baladi, eds.). STP 1026. ASTM, Philadelphia, Pa., 1989, pp. 313–322.
2. D. F. E. Stolle. Effect of Mechanical model on Back-calculated Pavement Modulus. *Canadian Journal of Civil Engineering*, Vol. 17, 1990, pp. 494–496.
3. R. L. Lytton, F. P. Germann, Y. J. Chou, and S. M. Stoffels. *NCHRP Report 327: Determining Asphaltic Concrete Pavement Structural Properties by Nondestructive Testing*. TRB, National Research Council, Washington, D.C., June 1990.
4. S. H. Carpenter and T. J. Freeman. Characterizing Premature Deformation in Asphalt Concrete Placed over Portland Cement Concrete Pavements. In *Transportation Research Record 1070*, TRB, National Research Council, Washington, D.C., 1986, pp. 30–41.
5. F. W. Jung and D. F. E. Stolle. Non-Destructive Testing with FWD on Whole and Broken AC Pavements. *Proc., Symposium*

- on *Nondestructive Deflection Testing and Backcalculation for Pavements*, August 19–21, 1991, Nashville, Tennessee (in preparation).
6. P. Ullidtz. *Pavement Analysis*. Elsevier, New York, N.Y., 1987.
 7. D. F. E. Stolle. Modelling of Dynamic Response of Pavements to Impact Loading—Technical Note. *Computers and Geotechnics*, Vol. 11, 1991, pp. 83–94.
 8. B. E. Sebaaly, M. S. Mamlouk, and T. G. Davies. Dynamic Analysis of Falling Weight Deflectometer Data. In *Transportation Research Record 1070*, TRB, National Research Council, Washington, D.C., 1986, pp. 63–68.
 9. F. P. Germann and R. L. Lytton. Temperature, Frequency, and Load Level Correction Factors for Backcalculated Moduli Values. In *Nondestructive Testing of Pavements and Backcalculation of Moduli* (A. J. Bush III and G. Y. Baladi, eds.). STP 1026. ASTM, Philadelphia, Pa., 1989, pp. 431–451.
 10. D. F. E. Stolle, D. Hein, and Y. Wang. Elastostatic Analysis and Backcalculation Estimates of Pavement Layer Moduli. *Proc., 1988 Annual Conference, Roads and Transportation Association of Canada*, Vol. 1, pp. C39–C59.
 11. D. M. Burmister. The General Theory of Stresses and Displacements in Layered Systems I. *Journal of Applied Physics*, Vol. 16, 1945, pp. 89–94.
 12. J. M. Golden. Strains and Displacements in Stochastic Stress Models. *Journal of Engineering Mechanics*, Vol. 114, No. 5, May 1988, pp. 876–886.
 13. F. W. Jung. *Interpretation of Deflection Basin for Real-World Materials in Flexible Pavements*. Report RR-242. Pavements and Roadway Section, Research and Development Branch, Ministry of Transportation of Ontario, Feb. 1990.
 14. A. H. Magnuson. A Comparison Study of Computer Predictions and Field Data for Dynamic Analysis of Falling Weight Deflectometer Data. Paper Prepared for Presentation at 70th Annual Meeting of the Transportation Research Board, Washington, D.C., 1991.
 15. J. S. Bendat and A. G. Piersol. *Engineering Applications of Correlation and Spectral Analysis*. John Wiley and Sons, New York, N.Y., 1980.
 16. S. Nazarian and K.H. Stokoe II. Nondestructive Evaluation of Pavements by Surface Wave Method. In *Nondestructive Testing of Pavements and Backcalculation of Moduli* (A. J. Bush III and G. Y. Baladi, eds.). STP 1026. ASTM, Philadelphia, Pa., 1989, pp. 119–137.
 17. F. E. Richard, J. R. Hall, and R. D. Woods. *Vibrations of Soils and Foundations*. Prentice-Hall Inc., Englewood Cliffs, N.J., 1970.
-
- Publication of this paper sponsored by Committee on Strength and Deformation Characteristics of Pavement Sections.